Fragmentation of stretched liquid ligaments

Philippe Marmottant[a)] and Emmanuel Villermaux[b)]
*IRPHE, Université de Provence, Technopôle de Château-Gombert 49, Rue Frédéric Joliot-Curie,
13384 Marseille Cedex 13, France*

The dynamics and fragmentation of stretched liquid ligaments is investigated. The ligaments are produced by the withdrawal of a tube initially dipping at a free surface. Time resolved high speed motion experiments reveal two different elongation behaviors, depending on the nondimensional number $\dot{\epsilon}t_\sigma$, ratio of the extension rate $\dot{\epsilon}$ to the capillary contraction rate $1/t_\sigma$, with t_σ the capillary time based on the tube diameter. For slow extensions (small $\dot{\epsilon}t_\sigma$) the liquid bridge linking the tube to the reservoir contracts above a critical elevation, eventually following a self-similar contraction before break-up. For fast extensions (large $\dot{\epsilon}t_\sigma$) the bridge takes the form of a cylindrical ligament, stabilized by the stretching motion. Whatever the elongation rate is, the ligament detaches from the surface at a time of order t_σ after the beginning of the extension. If only one small droplet is produced with a slowly stretched bridge, a set of droplets with distributed sizes is obtained from the break-up of the ligament submitted to a fast extension. We discover that an aggregative process comes into play between the blobs constitutive of the ligament as it fragments. The outcoming Gamma distribution describes well the observed broad drop size distributions. © *2004 American Institute of Physics.* [DOI: 10.1063/1.1756030]

I. INTRODUCTION

When a tube whose end dips into a liquid is rapidly withdrawn from a free surface it entrains a liquid ligament. This ligament is stretched between the tube end and the liquid free surface. It eventually separates from the liquid bulk, and fragments into dispersed droplets. This simple phenomenon is a paradigm for spray formation in many instances since the formation of a ligament is the last but one step before drop separation.

For example, the formation of spume, or the atomization of a liquid surface by a fast gas stream implies the formation of liquid ligaments stretched out of the surface, whose break-up determines the droplets sizes in the subsequent spray.[1,2] Other atomization processes, such as the break-up of high amplitude waves resulting from a Faraday excitation of a liquid surface, do have a transient state where stretched liquid ligaments are formed and eventually break into droplets.[3] More generally this paper also addresses the problem of the dynamics and breakup of the liquid column left in the wake of an object emerging from a liquid surface.

Liquid ligaments were extensively studied in their static form when suspended between two disks (liquid bridges). Their stability is experimentally assessed in the plateau tanks which compensate gravity by handling equal buoyancy liquids, in order to point out the effect of interfacial tension on stability. The influence of gravity on the shape and stability of the bridges was stimulated by microgravity experiments, and was analyzed for vertical bridges.[4,5] The shape of a vertical bridge was first solved, numerically,[6,7] on various axi-symmetric situations, including the two disk configuration, as well as the rod in free surface situation, where the bridge connects a disk and a liquid reservoir. Bridges are also formed during the detachment of a pendant drop from a faucet[8,9] and their stability accounts for the released drop size at very low flow rates (see the review of Eggers[10]). It was recently observed that the neck in between the faucet and the droplet takes the form of a long smooth cylindrical filament when the liquid has viscoelastic properties.[11] The break-up occurs in single location point, and the two remaining parts recoil quickly.

The effect of stretching on the stability of a liquid ligament was analytically investigated by Frankel and Weihs[12] for the case of inviscid liquid cylinder. With very viscous fluids, the stability was inspected by Henderson *et al.*[9] The extension of a liquid ligament is used to measure the extensional viscosity of non-Newtonian liquids. A constant elongation rate is imposed,[13] meaning an exponential extension of the length with time, while the axial forces on the end of the bridge are recorded. These measurements motivated numerical simulations of the stretching of a Newtonian fluid between a fixed disk and a moving disk, to establish the effect of viscosity on the diameter diminution and on the forces acting on the disks.[14]

Let us first examine the characteristic time scales involved in the ligament motion. The two main parameters are capillarity and elongation. The characteristic time of a capillary driven motion is the capillary time t_σ. At the scale of the diameter D of the tube it writes $t_\sigma = \sqrt{\rho_1 D^3/\sigma}$, with ρ the liquid density and σ the surface tension. The elongation is characterized by the rate $\dot{\epsilon} = (dH/dt)/H$, with H the elevation of the tube over the liquid surface (Fig. 1). The elongation and capillary rates are compared using the nondimen-

---

[a)]Present address: Department of Applied Physics, University of Twente, 7500 AE Enschede, The Netherlands.
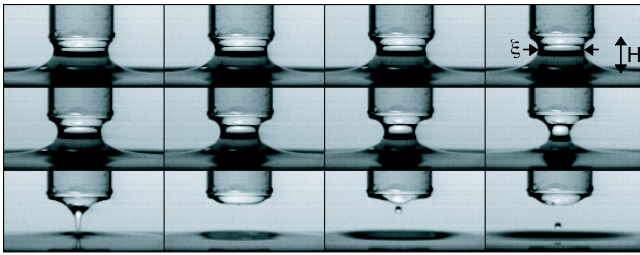[b)]Also at: Institut Universitaire de France.

2732

FIG. 1. Ligament contraction with a small elevation velocity (water, $D = 7$ mm, $\Delta t = 10.7$ ms).

FIG. 2. Minimum diameter and elevation before break-up ($\dot{\epsilon}t_\sigma \simeq 0.25$).

sional number $\dot{\epsilon}t_\sigma$, ratio of the imposed elongation rate $\dot{\epsilon}$, and the intrinsic capillary rate $1/t_\sigma$. In the present experiments, viscous effects are negligible compared to capillarity. The viscous diffusion time is $t_\nu = D^2/\nu$, with ν the viscosity of the liquid, and we can define a viscous rate with $1/t_\nu$. The relative magnitude of the viscous rate compared to the capillary rate is estimated by the Ohnesorge number Oh $= t_\sigma/t_\nu = \sqrt{\rho\nu^2/D\sigma}$. The Ohnesorge number when the tube exits out of the reservoir is 0.001 to 0.003 for water and ethanol ligaments, and 0.05 to 0.13 for the most viscous silicon oil, indicating a predominance of capillary-inertial forces on viscosity. The relative influence of gravity compared to stretching inertia is estimated by the Froude number $Fr = gH/(dH/dt)^2$, which in all the experiments was initially smaller than unity.

We will present in the following paper the evolution of the ligament in two limits. In the slow extension limit, $\dot{\epsilon}t_\sigma \ll 1$, the ligament has the shape of a bridge. When extension is fast, $\dot{\epsilon}t_\sigma \gg 1$, we will show that a long cylindrical part develops at the center of the ligament. We will eventually focus on the break-up of this extended columnar shape, and the subsequent droplet size distributions.

II. EXPERIMENTAL SET-UP

Liquid ligaments are produced from a liquid reservoir whose surface is at rest. The liquid reservoir has a diameter of 5 cm, which is large compared to the tube diameter. The glass tube is placed vertically so that its lower end dips slightly under the surface. The tube can then be quickly withdrawn manually, being careful to follow a vertical axis. A cable and a pulley were also used for that purpose. The maximum initial velocity we could obtain was about 2 m/s. Prior to the motion the tube was filled with the same liquid, and closed at the upper end so that the liquid does not fall. When some air pocket was trapped in the tube, only the bottom of the pipette was filled with liquid. However, there was no volume variation of the air pocket, and the bottom liquid
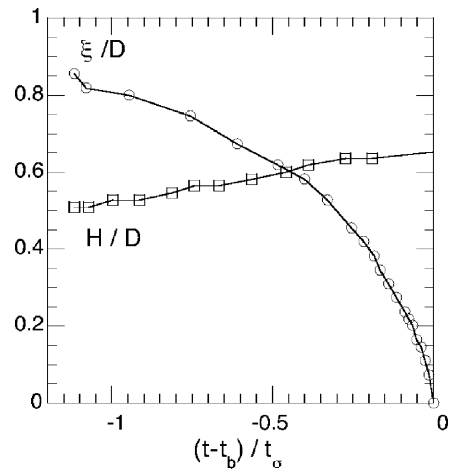
inside the pipette was entrained at the velocity of the pipette. A hollow tube was preferred to a plain rod because the liquid was not always properly attached to the latter, whose lower surface was subject to dewetting.

The outer (wetted) diameters of the tube were 1.4, 5, 7, and 15 mm. To explore the effects of fluid properties we used different liquids: distilled water, ethanol 95% ($\sigma \simeq 22$ mN/m), and two silicon oils ($\sigma \simeq 22$ mN/m), that are 5 and 20 times more viscous than water (see Table I). Images were recorded on a high speed motion camera, Kodak Hs Motion Analyzer 4540 MX (at the typical frequency of 2250 frames per second and images were 256 pixels wide).

III. DYNAMICS OF THE LIGAMENT

A. Slow extension $\dot{\epsilon}t_\sigma \ll 1$, volume contraction

When the liquid ligament is slowly extended, the bridge has time to adjust its shape to reach a stable equilibrium at each instant of time. Above a critical elevation no stable equilibrium exists and the bridge quickly contracts. It ultimately forms a thin cone over the plane surface (Figs. 1 and 2). After break-up the retraction of the cone creates a tiny satellite droplet.

The stability of the bridge, at a given elevation, is derived through the resolution of the Laplace equation, which states that the pressure difference between the inside and outside of the surface is $\Delta P = \sigma\kappa$, with κ the curvature of the surface. At equilibrium, for every altitude z the Laplace pressure equilibrates the hydrostatic pressure, and the Laplace equation writes $\sigma\kappa = -\rho g z$. The numerical resolution of this equation shows that it exists as a stable shape until a critical elevation of the tube, above which no solution

TABLE I. Liquid properties measured at 20 °C.

Liquid	Density ρ (kg m^{-3})	Viscosity ν (m^2 s^{-1})	Surface tension σ (N/m)
Water	993	1×10^{-6}	73×10^{-3}
Ethanol 95%	785	1.47×10^{-6}	21.5×10^{-3}
Silicon oil V5	913	5×10^{-6}	22.5×10^{-3}
Silicon oil V20	942	20×10^{-6}	22.5×10^{-3}
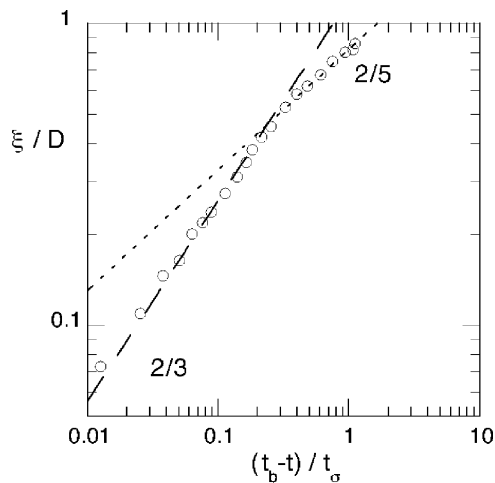
FIG. 3. Ligament thickness at the neck before break-up. Lines: power laws.

FIG. 4. Contraction regimes: initial contraction of the whole volume and contraction of the central part.

exists.[15] This behavior is also found when considering the classical case of the equilibrium shape of a film between two rings of equal diameter: it is a catenoid, that exists only when the distance between the rings is smaller than a critical value, of about $0.66D$. On the contrary, in the present case the maximum elevation always depends upon the relative influence of gravity over capillarity,[15] which is expressed by the Bond number $\mathrm{Bo}=\rho g D^2/\sigma$. With the tested diameter $D=7$ mm, the Bond number is 6.9 and according to the numerical results of Padday and Pitt[15] the critical elevation is about $1.3 l_\sigma$, or $0.49D$. When tube diameter D is very large compared to the capillary length $l_\sigma=\sqrt{\sigma/\rho g}$, meaning that the Bond number $\mathrm{Bo}=(D/l_\sigma)^2$ is very large, the critical elevation tends to $2 l_\sigma$.

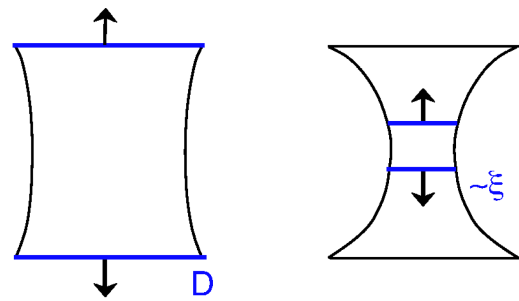The slow extensional motion therefore leads the bridge towards an unstable shape, and results in the bridge pinch-off. The minimum diameter ξ of the bridge as a function of time before break-up $t-t_b$ shows two regimes of contraction (Fig. 3).

Those regimes are linked to the different geometries of the flow during the contraction: initially the whole volume is contracted by capillary forces (since excess capillary pressure is equally distributed), while prior break-up the pinch-off area volume is dominantly contracted (since capillary pressure is concentrated in this area), see the illustration of Fig. 4.

An analysis of the characteristic volumes involved in the contraction enlightens the power dependence of the bridge diameter as a function of time before break-up. Initially, the displaced volume scales as $V\sim\xi^2 D$ and exits through the lower surface of order $S\sim D^2$ (the bridge shape being quasi-symmetric). Since the pressure at the center is $2\sigma/\xi$ and vanishes at the free surface of the reservoir, we can estimate the fluid velocity at exit, from the steady flow Bernoulli equation: $u\sim 2\sqrt{\sigma/\rho\xi}$. The conservation of volume $dV/dt=-uS$ yields

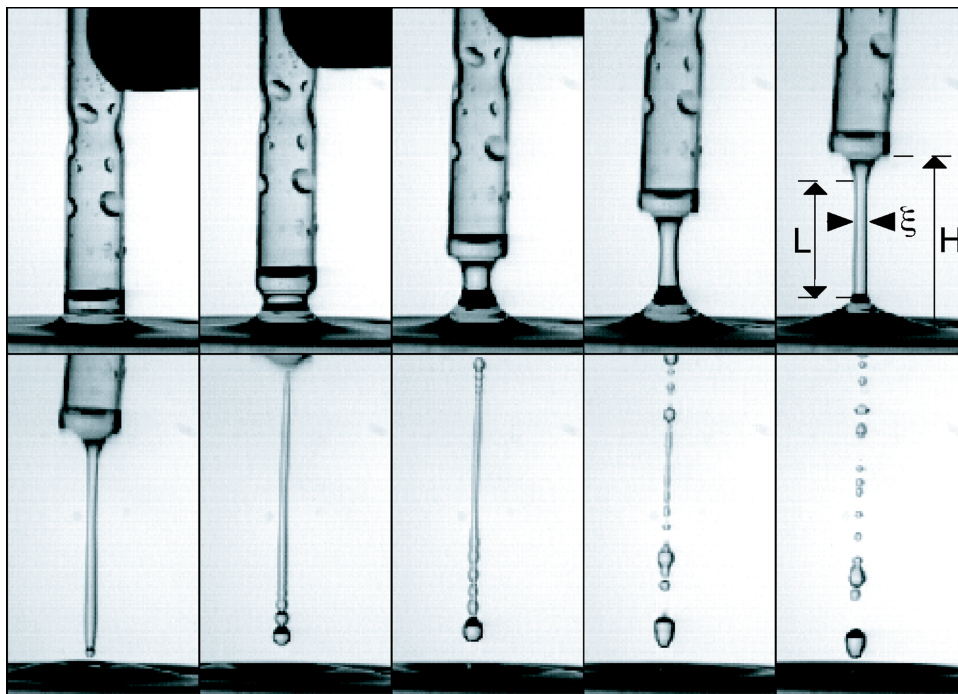
FIG. 5. Fast elongation of a liquid water ligament, capillary tube of diameter $D=7$ mm, time intervals $\Delta t=4.5$ ms.

$$\frac{\xi}{D} \sim \left(1 - \alpha \frac{t}{t_\sigma}\right)^{2/5}, \tag{1}$$

with α a constant of order 1 that would be derived by a detailed analysis of the flow geometry.

Eventually, just prior break-up, the motion is essentially concentrated in a region of volume $V \sim \xi^3$, and empties through a surface of order $S \sim \xi^2$. The motion is self-similar.[16] These estimates of exit velocity and volume conservation then lead to

$$\frac{\xi}{D} \sim \left(1 - \beta \frac{t}{t_\sigma}\right)^{2/3}, \tag{2}$$

with β another constant of order 1. These two regimes are indeed displayed when plotting ξ versus $t_b - t$ (Fig. 3).

The pinch-off of a symmetric film bridging two circles, exposed by Cryer *et al.*[17] and detailed numerically by Chen and Steen[18] on the inviscid approximation, also displays the same $-2/3$ regime during the contraction of the central part. In this exactly symmetrical configuration (where gravity is not acting), thus different from the present study, the contraction regime is self-similar only on a limited range of time. The central part contracts into a tiny cylinder instead of the present cone, and then pinches off on two symmetric points, which leads to the formation of the satellite droplet. These two pinch-off points are then asymmetric because they take place between a cylindrical part and a conical part, and they behave in a truly self-similar way until break-up.

We have to emphasize that the above discussion has been conducted in the inertial limit which does not hold at infinitely small scales, when $\mathrm{Re} = \sqrt{\sigma \xi / \rho \nu^2}$ becomes small. Viscous effects then become significant as well at the very last moment of the contraction, but the time period of their predominance is short[19] compared to the overall pinching period t_σ.

B. Rapid extension $\dot{\epsilon} t_\sigma \gg 1$, columnar shape

When the extension is rapid compared to the initial capillary time, the central part of bridge takes the shape of a liquid column. This section will focus on the dynamics of this column, for its break-up is at the origin of a set of droplets (Fig. 5).
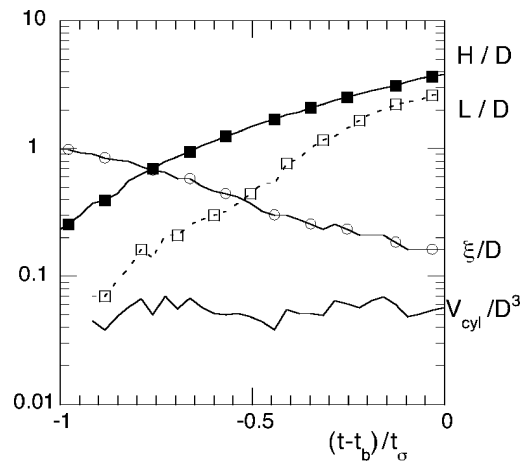
FIG. 6. Dimensions of the liquid column during its development (initially $\dot{\epsilon} t_\sigma \simeq 5$).

1. Observations

The lengths were measured on the high speed image sequences; we distinguish the diameter of the central part ξ, the elevation of the tube over the free surface H, and the length of the approximately cylindrical shape L (where the diameter is ξ within one pixel). These measurements show that the elevation H and the columnar part height L do not have a parallel evolution (Fig. 6). While the growth rate of imposed elevation H is decreasing (after an initiation period where H is close to an exponential), the growth rate of the columnar length L remains constant. Their rate of growth, shown in the log-lin diagram of Fig. 6, is nevertheless initially comparable. Another remarkable feature is that the volume of the cylinder, derived by $V_{\mathrm{cyl}} = \pi \xi^2 L/4$, remains constant during the extension.

Various emerging velocities were applied [Fig. 7(a)], and they all show that the columnar length L is initially a small fraction of the height H, that this proportion increases, and that the two lengths become eventually very close just prior to break-up. The diameter ξ of the column decreases more rapidly for fast extensions but eventually all the curves follow the same decay [Fig. 7(b)]. At the opposite of the slow extension case, it is noticed that the central part is destabilized and breaks up only after a pinch-off near the tube end or near the reservoir. The diameter ξ therefore does not vanish at the time of first break-up.
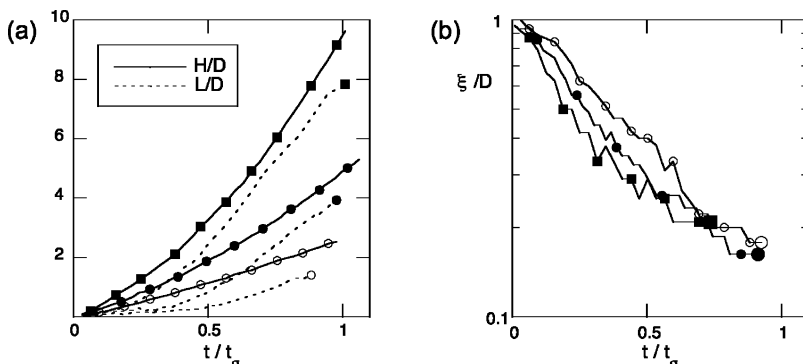
FIG. 7. (a) Different elongation velocities of H and the resulting evolution of L. Last point is break-up (water, $D = 5$ mm). (b) The corresponding thickness of the ligament.
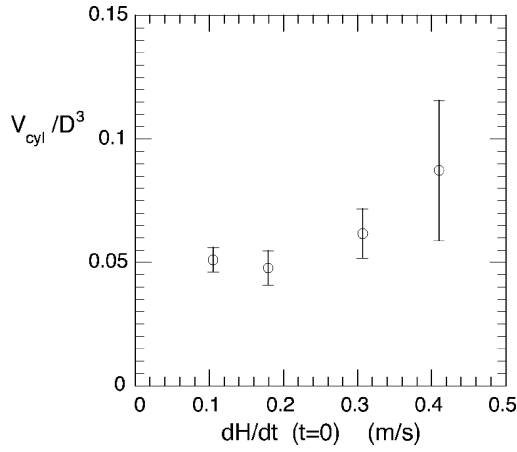
FIG. 8. Volume of the cylindrical part as a function of the initial velocity of the tube when it exits (ethanol, $D = 5$ mm).

2. Entrained volume in the column

The volume entrained in the cylinder depends on the initial conditions of the tube motion, that is the initial immerged depth under the surface, and the acceleration given to the liquid before the pipette exits out of the surface. It can be noticed that a higher velocity dH/dt at exit produces a larger ligament (Fig. 8). As we cannot deduce the initial conditions from our measurements, we will take the entrained volume as an initial parameter. Measurements with various liquids show that this volume is typically of order $0.065D^3$. This volume can be expressed using the diameter d_0 it would have if gathered in a single sphere such that

$$V_{\text{cyl}} = \pi \xi^2 L/4 = \pi d_0^3/6. \tag{3}$$

The diameter d_0 is typically of order $0.5D$.

3. The stretching motion damps the column contraction

We model the inviscid motion of the liquid column, assuming it is a cylinder extending at a constant rate with $L = L_0 \exp(\dot{\epsilon} t)$. The extension rate of L is chosen to be the same as the extension rate of H, as suggested by the observations when considering the beginning of the extension.

The liquid can flow out of the column through the attached end of surface $S \simeq \pi \xi^2/4$ at the velocity u. The exit velocity can be estimated using the Bernoulli approximation between the central part of the cylinder of capillary pressure $2\sigma/\xi$ and the exit surface, where capillary pressure vanishes,

as was done in the previous section where we had $u = 2\sqrt{\sigma/\rho\xi}$. The continuity equation $dV_{\text{cyl}}/dt = -uS$ writes

$$\frac{d(\xi^2 L)}{dt} = -2\sqrt{\frac{\sigma\xi^3}{\rho}} \tag{4}$$

which solves in

$$\frac{\xi}{D} = \left(1 - \frac{4}{5}\frac{D}{L_0}\frac{1 - e^{-\dot{\epsilon}t/2}}{\dot{\epsilon}t_\sigma/2}\right)^{2/5} e^{-\dot{\epsilon}t/2}. \tag{5}$$

For the vanishing stretching rate ($\dot{\epsilon} \to 0$) we find again the solution for the initial contraction of the bridge [Eq. (1)]: $\xi/D = (1 - \alpha t/t_\sigma)^{2/5}$, with $\alpha = \frac{4}{5}(D/L_0)$.

For a large stretching rate of the columnar part ($\dot{\epsilon} t_\sigma \gg 1$), the diameter follows $\xi/D \simeq \exp(-\dot{\epsilon}t/2)$, which means that the volume undergoes contraction without breaking nor emptying (since $L\xi^2 \sim \text{cst}$). A fast stretching motion damps the capillary contraction and the volume is conserved.

The transition between those two cases is displayed in Fig. 9 for the diameter and the volume. The volume contraction is less than 20% at $t = t_\sigma$, when $\dot{\epsilon} t_\sigma = 10$.

4. Motion of the column

The initial extension rate of the column height L is close to extension rate $\dot{\epsilon}$ of the elevation H. This rate is always large compared to the capillary rate, $\dot{\epsilon} t_\sigma > 5$ in the present experiment, the previous section therefore shows that it is small enough to insure an evolution at constant volume. Since the liquid is stretched into a column of homogenous radius it is not subjected to a gradient of capillary pressure anymore on its surface. The column is only pulled by the capillary forces at its upper end (Fig. 10).

We model here the motion assuming a cylindrical shape all along the ligament. To remain cylindrical, the flow at a point (r, z) in the column has to be extensional, $(u_z, u_r) = (z/L \times \dot{L}, -r/2L \times \dot{L})$. The momentum on the vertical axis is $p_z = \int_V \rho u_z dV = \rho V \dot{L}/2$.

The cylinder is pulled by the capillary force acting on the perimeter of the upper section. We have also to consider the liquid pressure acting on the surface of the upper section, and the gravity acting on the total volume. The momentum equation writes, after projection on the vertical axis,

$$\tfrac{1}{2}\rho V \ddot{L} = 2\pi\sigma r - \Delta p \pi r^2 - \rho g V, \tag{6}$$

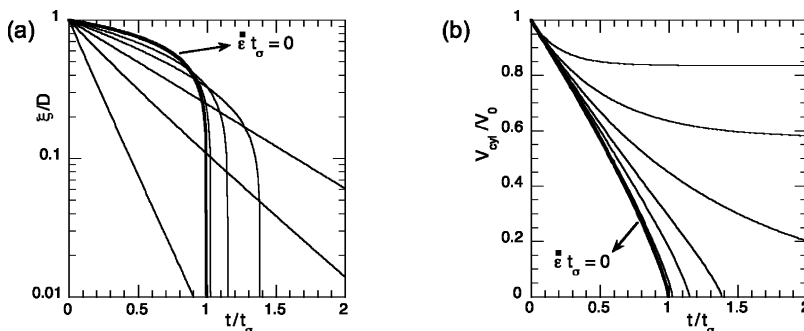(a) $\dot{\epsilon} t_\sigma = 0$

(b)

FIG. 9. Ligament diameter (a) and volume (b) of a stretched cylinder of length $L = L_0 \exp(\dot{\epsilon} t)$, with increasing stretching rates: $\dot{\epsilon} t_\sigma = 0$ (thick line, no stretching), 0.1, 0.5, 1, 2, 4, 10. The diameter evolution is increasingly closer to $\xi/D = \exp(-\dot{\epsilon}t/2)$ for large stretching rates.
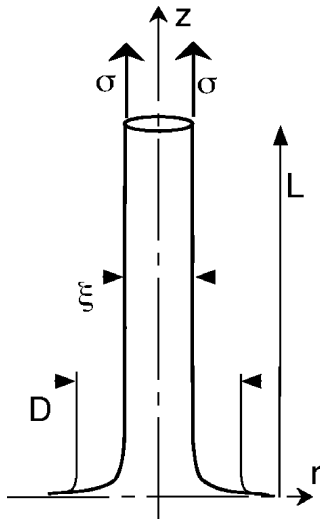
FIG. 10. Stretching of the cylinder by the pipette.

FIG. 12. Decay rate of ligament diameters. Water (full circles), ethanol (open circles), silicon oils (crossed circles).

with the radius $r = \xi/2$. The difference between the inner and outer pressure, Δp, is here the capillary pressure σ/r acting on the cylinder. The volume is $V = \pi r^2 L$.

This equation is conveniently written in units of d_0 for lengths (introducing the nondimensional length $L^* = L/d_0$) and in units of the capillary time $t_0 = \sqrt{\rho d_0^3/\sigma}$ for the time (introducing $t^* = t/t_0$) giving

$$\frac{d^2 L^*}{dt^{*2}} = \alpha \, \frac{1}{\sqrt{L^*}} - 2 \, \mathrm{Bo}, \qquad (7)$$

with $\alpha = 2\sqrt{6}$. The Bond number $\mathrm{Bo} = \rho g d_0^2/\sigma$ is small in our experiments (always smaller than 1), we will neglect its influence in the following. Equation (7) integrates into the implicit solution $(2\alpha\sqrt{L^*} - a)\sqrt{4\alpha\sqrt{L^*} + a} + b = 6\alpha^2 t^*$, where a and b are integration constants determined by the initial conditions. It is plotted in Fig. 11 with the initial condition $\xi = d_0$ and several initial velocities expressed as a function of the capillary velocity $v_0 = d_0/t_0$. When the ini-
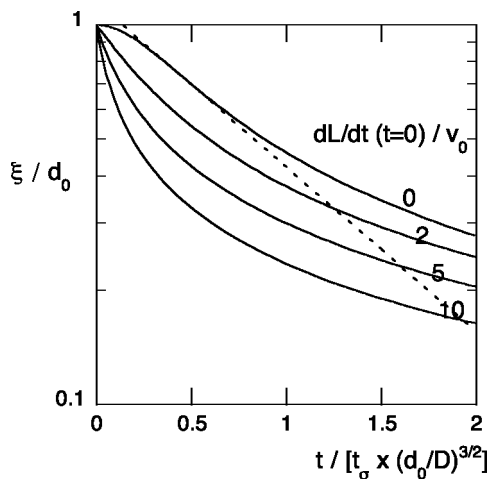
tial velocity is small in comparison with v_0, the diameter ξ as a function of time is very close, in the range $[0 \cdots t_0]$, to an exponential whose decay time is t_0:

$$\frac{\xi}{D} \propto e^{-t/t_0} \quad \text{with} \quad t_0 = t_\sigma (d_0/D)^{3/2}. \qquad (8)$$

The characteristic time t_0 differs from t_σ since the traction is performed by capillary forces acting on the ligament perimeter, of order d_0, different from the tube diameter D.

The diameter versus time curves obtained with various experiments of ethanol and water all show a final exponential decay [see Fig. 7(b) for a typical case].

The model obtained directly from the equation of motion thus describes correctly the extension until the time t_0 (with $t_0 < t_\sigma$), but underestimates it for larger times.

The final characteristic decay time $\xi/(d\xi/dt)$ is close to $t_0 = t_\sigma (d_0/D)^{3/2}$, as shown in Fig. 12, except for the diameter $D = 15$ mm, which was, because of its larger size, subject to gravity.

IV. LIGAMENT BREAK-UP

A. Time of break-up

Ligaments undergoing a fast extension first break up at their extremities, either on the top near the tube, or on the bottom near the liquid container, or both at the same time. Then the whole column fragments into droplets. The explanation of this preferential location for the first break-up resides in the fact that the central part is stretched, smoothing the surface curvature to a constant value $\kappa = 1/\bar{R}_1 + 1/\bar{R}_2 = 2/\xi$ (the principal curvature in the plane orthogonal to the ligament axis is $1/\bar{R}_1 = 2/\xi$, the other is $1/\bar{R}_2 \to 0$). There is no gradient of capillary pressure in this region. However, at the ligament ends, the surface bridging the cylindrical part to the tube or to the reservoir has a vase shape, and the curvature is rapidly decreasing in the direction away from the cylindrical part (since $1/\bar{R}_1$ decreases, and $1/\bar{R}_2$ also decreases, becoming negative). The variation of the curvature

FIG. 11. Diameter of the ligament stretched by capillarity for different initial velocities. Dotted line: exponential fit.
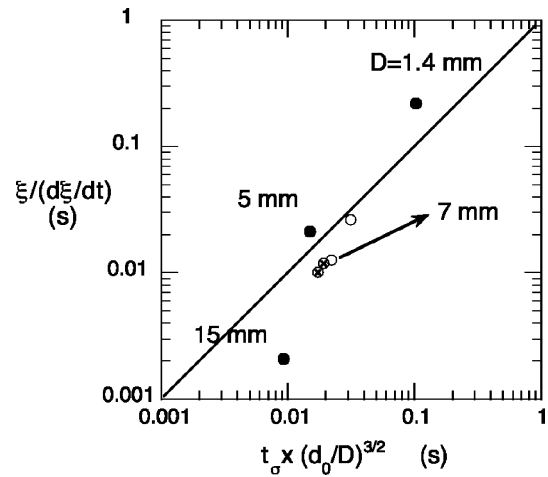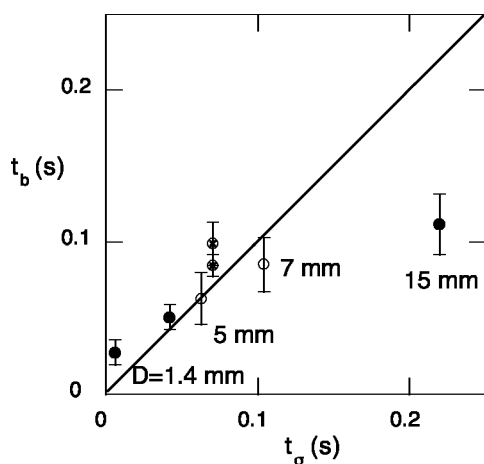
2738   Phys. Fluids, Vol. 16, No. 8, August 2004

P. Marmottant and E. Villermaux
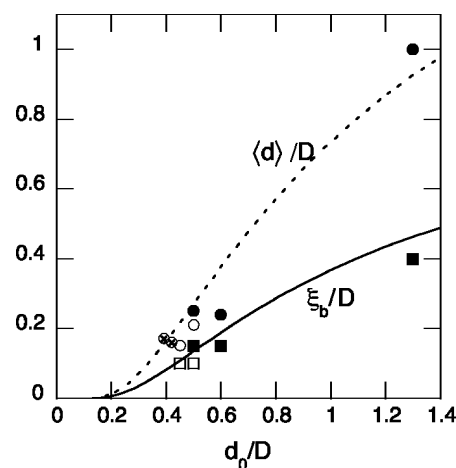

FIG. 13. Time of first break-up.

FIG. 14. Mean diameter of the droplets (circles, same symbols as Fig. 12), diameter of the ligament before break-up (squares, full for water, open for ethanol). Continuous line: expected diameter ξ_b of the ligament before break-up; dotted line: $2\xi_b$.

accounts for a variation of capillary pressure, that displaces away from the center the liquid contained in the ligament end: this is the place of pinch-off onset.

The break-up time is therefore fixed by the contraction of the ends: it scales like the characteristic capillary time t_σ based on the initial diameter, as did the break-up time of the bridge undergoing a slow extension. The recorded time of first break-up, t_b does not significantly depend on the initial withdrawing velocity (which varied between 0.5 m/s and 2 m/s). It is always close to $t_b=1.0t_\sigma$, see Fig. 13. The largest diameter, 15 mm, breaks sooner: in addition to the above-mentioned effect of gravity it was subjected to surface undulations from the beginning of the stretching attributed to a largest initial Reynolds number ($Re_H=D\dot{H}/\nu\sim10^4$). The silicon oil ligaments breaks in a slightly longer time, consistent with a viscous damping of the capillary pinch-off instability. Indeed the stability analysis[10,20] shows that the characteristic time of growth of perturbations on a liquid cylinder is $t_\sigma=\sqrt{\rho_1\xi^3/\sigma}\times f(Re)$, with $Re=\sqrt{\xi\sigma/\rho\nu^2}$. For large Re, the function $f(Re)$ is close to unity, but for small Re it becomes larger than unity,[2] meaning that viscous effects increase the pinch-off time of the liquid cylinder. For the same reason, the contraction of the ends of small diameters ligaments slows down compared to the pure inviscid estimation.

B. Mean droplet size

Once the ligament has detached from the liquid bulk, embedding a volume V, it may either gather itself into a unique droplet of size d_0 such that $V=\pi d_0^3/6$ (for small aspect ratio H/ξ of the ligament), or either break into several droplets. When the ligament is infinitely long, smooth, and uniform, the characteristic droplet size is the ligament thickness ξ_b. In the present case, the average drop size $\langle d\rangle$ is in between these two limits.

Although this is not generally the case (for instance with airstream elongated ligaments[2]), the large aspect ratio ligaments produced in the present experiments are close to this uniform limit. The average diameter is about two times ξ_b. Using Eq. (8) at $t=t_\sigma$, we have $\xi_b/D\sim\exp(-(d_0/D)^{-3/2})$. A good approximation of $\langle d\rangle$ is $2\xi_b$ (Fig. 14), the factor 2

being similar to the one that holds for the break-up of a smooth cylinder.[10]

However, the ligaments are not fully described by this limit because the distribution of sizes is not a uniform distribution centered around ξ_b. Understanding the full shape of the distribution is thus necessary.

C. Fragmentation

After pinch-off of the ligament ends, the whole cylindrical column destabilizes (Fig. 5). The ligament is disturbed by transient surface undulations, and the liquid volumes constitutive of the ligament interact before complete separation. The droplet sizes in the final state are broadly distributed (see Fig. 15).

The randomness of the outcoming droplet size is illustrated by the images of Fig. 16, showing the size distributions after the break-up of different ligaments prepared in similar conditions. It can be pointed out that droplet distributions vary a lot. There is no ordered or deterministic size sequence along the vertical axis.

A broad distribution of sizes is typical of fragmentation process involving uncontrolled break-ups. This phenomenon has been known for a long time and goes beyond the particular case of sprays. It has prompted several interpretations.

(i)   A first class of models was introduced by Kolmogorov.[21,22] The overall breakup is visualized as a sequential process where mother drops give rise to daughter drops which themselves break into smaller drops. In this cascade processes, a particle of initial volume v_0 breaks, after n steps of the cascade into a family of drops of volume $v_n=v_0\Pi_{i=1}^n\alpha_i$, where α_i are random multipliers smaller than unity. The logarithm of the volumes is thus distributed Normally, leading a log-normal distribution for the volumes themselves. A variant of this model is to consider a normal distribution of cascade steps n at fixed $\alpha=1/2$. In this scenario, the arrow of the evolution is directed towards ever smaller sizes.
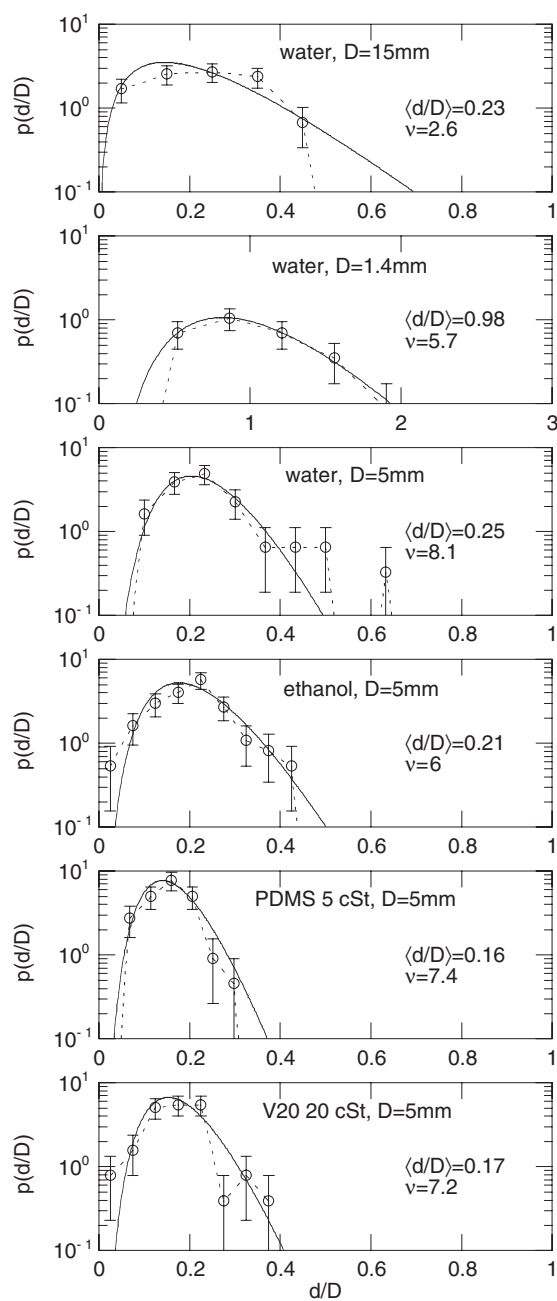
FIG. 15. Droplet size distribution after break-up. Fit with a *gamma* distribution of parameter ν, see Eq. (13).
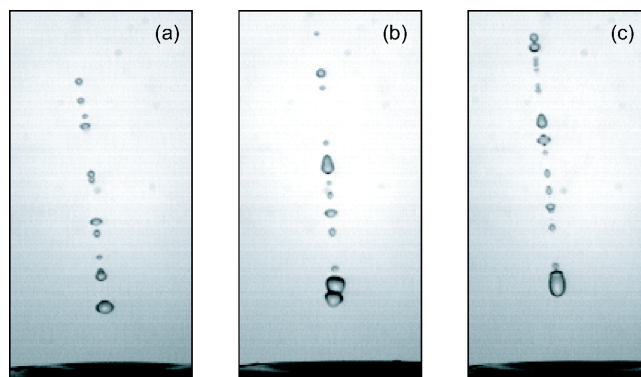

FIG. 16. Ligament just after complete fragmentation in three different experiments with comparable elongation velocities, slightly increasing from (a) to (c). The sequence of droplet sizes along the ligament vary a lot from experiment to experiment (water, $D = 5$ mm).

At the opposite of fragmentation, the dynamical processes of aggregation of an ensemble of small elementary particles was accounted for by Smoluchowski.[28] Based on the assumption that the probability of encounter and aggregation between two aggregates is independent of sizes, the evolution of the number of aggregates of a given size can be estimated. It provides a kinetic equation for the evolution of the number of particles of a each size. This equation asymptotically produces decreasing exponential distributions.

Somewhat paradoxically, the break-up of a ligament in droplets involves aggregative processes during the fragmentation of the ligament. Indeed the high speed time resolved movies show complex rearrangements of liquid volumes along the ligament, forming bigger and bigger sizes prior to break-up. These rearrangements have various sources as the travel of capillary waves generated by the recession of the extremities after pinching, the transient growth of the capillary instability, the remnant motions in the liquid bulk. The classical Rayleigh instability of a quiescent liquid thread of uniform thickness, which would create a succession of droplets of equal sizes, therefore does not hold. The random break-up description, which would give exponential statistics for the droplet volumes, does not apply either because of the interactions along the ligament.

The ligament consists of a linear succession of liquid blobs that undergo a continuous interplay during the destabilization. The evolution of their size distribution ultimately rules the droplet size distribution, when the liquid blobs detach from each other. Let $n(d,t)$ be the distribution of liquid blobs on the ligament: the number of blobs whose length is within d and $d + \mathrm{d}d$ at time t is $n(d,t)\mathrm{d}d$. We describe the random rearrangements of the liquid in the ligament by the motions of ν independent layers [see Fig. 17(b)]. We denote by $q(d',t)$ the distribution of the layer thickness d' in each layer.

Since the layers are adjacent to each other in a section, each blob is composed of ν sub-blobs, and the mean diameter of a liquid blob is $\langle d \rangle = \nu \langle d' \rangle$. The average thickness of the layers $\langle d \rangle / \nu$ reflects the characteristic mean free path of the liquid motions in the ligament.

Because of the random liquid motions in the ligament,

(ii)   The second class of approach considers the random splitting of an initial volume in various disjointed elements, in one step. Essentially inherited from the methods developed for the kinetic theory of gases[23] and the physics of polymers,[24] the idea is to visualize a given volume as a set of elementary bricks, and to compute the most probable distribution of the disjointed clusters incorporating the bricks.[25–27] The most probable distribution is the one that corresponds to the largest number of combinations (or maximum entropy) and yields a Poisson law for the distribution of the volumes. This description is purely combinatory, and does not account for any interaction between the clusters as they separate.
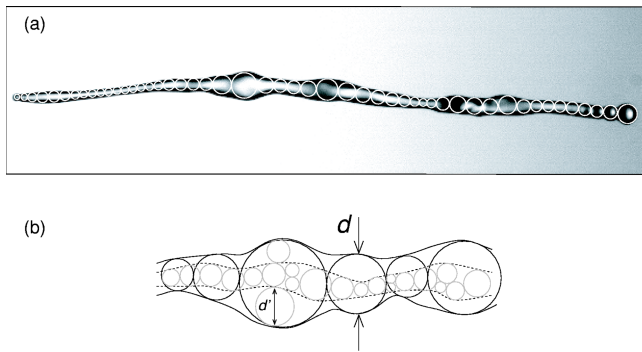
(a)

(b)

FIG. 17. (a) Subdivision of the ligament in liquid blobs. (b) The internal rearrangements of liquid in the ligament are modeled by layers of sub-blobs of diameter d'. Their superposition accounts for the size d of the blobs along the ligament.

the sub-blobs of a layer overlap and merge. If we assume they interact randomly with each other in a layer, with no correlation between their size, the probability of an interaction between two sub-blobs is $Kq(d'_1)q(d'_2)dd_1dd'_2$, for sizes that are within d'_i and $d'_i+dd'_i$ ($i=1,2$), and produces a new sub-blob of thickness $d'_1+d'_2$. Since the capillary processes are driven at the characteristic time $t_\xi=\sqrt{\rho\xi^3/\sigma}$ based on the initial average blob size $\xi=\langle d\rangle_0$, the interaction frequency is of order $K\sim 1/t_\xi$. The evolution of the distribution thus follows

$$\partial_t q(d',t)=-Kq(d',t)Q(t)+\alpha Kq(d',t)^{\otimes 2}, \qquad (9)$$

with $Q=\int_0^\infty q(d',t)dd'$ the number of liquid sub-blobs and $q^{\otimes 2}=\int_{d'=d'_1+d'_2}q(d'_1)q(d'_2)dd'_2$ the autoconvolution of the distribution. The constant α is determined by the constraint of overall volume conservation. The first term on the right-hand side of the kinetic Eq. (9) is the rate of loss due to aggregation, and the second term the rate of formation of new sizes by interaction among the particles.

The blobs on the ligament are the superposition of ν independent layers, and d the sum of ν independent layers of thickness d'. The *probability* distribution of the diameter d is n/N, with $N=\int_0^\infty n(d,t)dd$ the total number of blobs con-

stitutive of the ligament. It is therefore the probability of a sum of independant variables whose probability distribution is q/Q, and for a given time t we have

$$\frac{n}{N}=\left(\frac{q}{Q}\right)^{\otimes\nu}. \qquad (10)$$

The evolution of the distribution $n(d,t)$ is then, after a derivation using the Laplace transform of the last two equations,

$$\partial_t n(d,t)=-Kn(d,t)N(t)^{\gamma-1}+\beta Kn(d,t)^{\otimes\gamma}, \qquad (11)$$

with $\gamma=1+1/\nu$, and β a parameter whose value is deduced from the conservation of the total volume. This equation is a generalization of the Smoluchowski equation to an arbitrary number γ of entities involved at each interaction.

The conservation of the available volume $V=d^3n(d,t)dd$ determines the prefactor β in Eq. (11) which is $\beta=1/(3\gamma-2)$. The interaction parameter γ is set by the compatibility of Eq. (11) with the initial distribution of blobs by

$$\gamma=\langle d^2\rangle_0/\langle d\rangle_0^2. \qquad (12)$$

A smooth ligament of constant thickness has $\gamma=1$ and a corrugated ligament is such that $\gamma>1$.

The asymptotic solution of Eq. (11) for $p=n(d,t)/N(t)$ is a *gamma* distribution of order $\nu=1/(\gamma-1)$. The very mechanism goes back to the discovery by Smoluchowski that aggregative systems like $q(d',t)$ in Eq. (9) evolving by self-convolution have the property to generate asymptotically exponential distributions.[28] Here the asymptotic distribution of blobs $p(d,t)$ is a convolution of ν of these exponential distributions, providing

$$p(x=d/\langle d\rangle)=\frac{\nu^\nu}{\Gamma(\nu)}x^{\nu-1}e^{-\nu x}, \qquad (13)$$

where $\langle d\rangle=\int dn(d,t)dd/N(t)$ is the current average blob diameter. This distribution varies from an exponential when $\nu=1$ to a Gaussian distribution when ν is large. It fits well the final break-up distribution, which displays an asymmetric bell shape, with an exponential wing at large diameters (see Fig. 15).
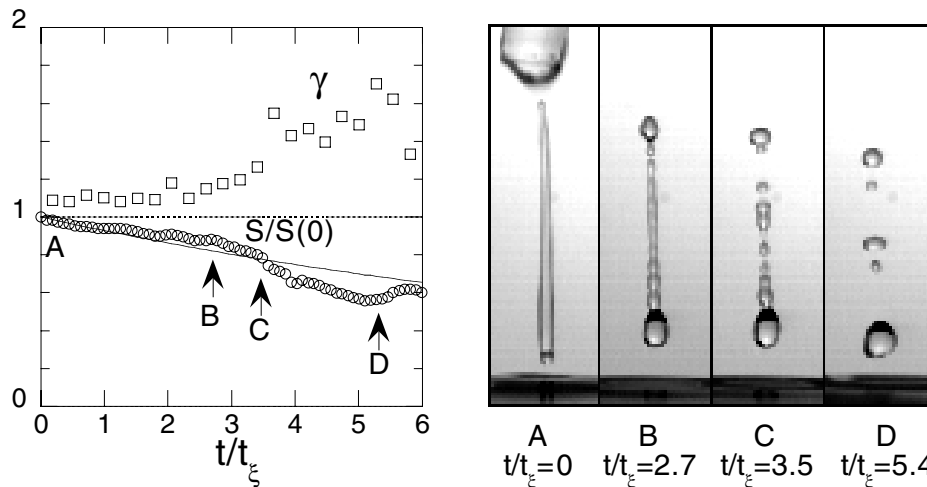

FIG. 18. Left: Evolution of the roughness γ of the ligament (squares) and of the surface $S/S(t=0)$ (circles) as a function of the time in units of the capillary time t_ξ. The continuous line is a prediction of the model for $S(t)$. Right: images of the ligament at four different times. Water, $D=5$ mm.

The rearrangements and coalescence of liquid blobs reduce their total number. According to Eq. (11) this number decreases in time as $N(t)/N(0) = [1 + N(0)^{1/\nu} Kt/\nu(1 + \nu/3)]^{-\nu}$ as well as the surface area of the blob [second moment of the distribution $n(d,t)$] which goes like $S \sim N^{1/3}$.

The extraction of the contours of a breaking ligament from the high speed sequences provides the distributions $m(\xi,t)$ of the thickness ξ along the ligament as a function of time, from which the distribution $n(d,t) = m(d,t)/d$ of spheres covering the ligaments as a bead on a necklace can be computed [see Fig. 17(a)]. From this measure we obtain the distribution of the liquid blobs $p(d,t)$, their net surface $S(t) = N(t)\int d^2 p(d,t) \mathrm{d}d$, and the roughness parameter $\gamma = \langle d^2 \rangle / \langle d \rangle^2$ (see Fig. 18 for a typical case).

After the ligament has detached from the liquid bulk and during its rearrangement phase while it is still connected (images A and B in Fig. 18), the roughness is fairly constant ($\gamma \simeq 1.1$). It then increases when the ligament breaks into droplets. The order of the *gamma* distribution $\nu = 1/(\gamma - 1) \simeq 10$ predicted during the initial phase is in agreement with the one deduced from the shape of the droplet size distribution after break-up ($\nu = 8.1$ for the same conditions, as shown in Fig. 15). The expected evolution of S with $\nu \simeq 10$ gives the general decreasing trend as well. The surface is decreasing faster at the moment of the droplet separation (image C). Then the surface tends to a final constant value (image D).

V. CONCLUSION

The experimental study we have conducted with low viscosity liquids shows that a liquid ligament stretched out of a free surface displays two types of behaviors. For a slow extension ($\dot{\epsilon} t_\sigma \ll 1$) it contracts as a bridge, while for a fast extension ($\dot{\epsilon} t_\sigma \gg 1$) it is stretched as a cylindrical ligament whose volume is conserved.

The ligament breaks up on a time t_σ based on the diameter of the tube, after the beginning of the extension, whatever the stretching rate is. For large stretching rates, the pinch-off is first located on the liquid connections to the tube or the reservoir, and not on the cylindrical ligament. The ultimate break-up of the ligament produces large distributions of droplet sizes. The broadness of the distribution is a consequence of the random interaction of the liquid in motion along the ligament, an interaction of an aggregation type. This process, in which large blobs grow at the expense of smaller ones produce blob size distributions stable by self convolution, namely *gamma* distributions, which ultimately set the overall drop size distribution.

ACKNOWLEDGMENTS

[1] P. Marmottant and E. Villermaux, "Ligament mediated drop formation," Gallery of Fluid Motion, Phys. Fluids **13**, S7 (2001).

[2] P. Marmottant and E. Villermaux, "On spray formation," J. Fluid Mech. **498**, 73 (2004).

[3] B. Vukasinovic, A. Glezer, and M. Smith, "Vibration-induced droplet atomization," Gallery of Fluid Motion, Phys. Fluids **12**, S12 (2000).

[4] J. Mesguer and A. Sanz, "Numerical and experimental study of the dynamics of axisymmetric slender liquid bridges," J. Fluid Mech. **153**, 83 (1985).

[5] J. Padday, G. Petré, C. Rusu, J. Gamero, and G. Wozniak, "The shape stability and breakage of pendant liquid bridges," J. Fluid Mech. **352**, 177 (1997).

[6] C. Huh and L. E. Scriven, "Shapes of axisymmetric fluid interfaces of unbounded extent," J. Colloid Interface Sci. **30**, 323 (1969).

[7] J. Padday, "The profiles of axially symmetric menisci," Philos. Trans. R. Soc. London, Ser. A **269**, 265 (1970).

[8] D. Peregrine, G. Shoker, and A. Symon, "The bifurcation of liquid bridges," J. Fluid Mech. **212**, 25 (1990).

[9] D. Henderson, H. Segur, L. B. Smolka, and M. Wadati, "The motion of a falling liquid filament," Phys. Fluids **12**, 550 (2000).

[10] J. Eggers, "Nonlinear dynamics and breakup of free-surface flows," Rev. Mod. Phys. **69**, 865 (1997).

[11] L. B. Smolka and A. Belmonte, "Drop pinch-off and filament dynamics of wormlike micellar fluids," J. Non-Newtonian Fluid Mech. **115**, 1 (2003).

[12] I. Frankel and D. Weihs, "Stability of a capillary jet with linearly increasing axial velocity (with application to shaped charges)," J. Fluid Mech. **155**, 289 (1985).

[13] S. H. Spiegelberg, D. C. Ables, and G. H. McKinley, "The role of end-effects on measurements of extensional viscosity in filament stretching rheometers," J. Non-Newtonian Fluid Mech. **64**, 229 (1996).

[14] S. Gaudet, G. McKinley, and H. Stone, "Extensional deformation of Newtonian liquid bridges," Phys. Fluids **8**, 2568 (1996).

[15] J. Padday and A. Pitt, "The stability of axisymmetric menisci," Philos. Trans. R. Soc. London, Ser. A **275**, 489 (1973).

[16] J. B. Keller and M. J. Miksis, "Surface tension driven flows," SIAM (Soc. Ind. Appl. Math.) J. Appl. Math. **43**, 268 (1983).

[17] S. A. Cryer and P. H. Steen, "Collapse of the soap-film bridge: Quasistatic description," J. Colloid Interface Sci. **154**, 276 (1992).

[18] Y.-J. Chen and P. H. Steen, "Dynamics of inviscid capillary breakup: collapse and pinchoff of a film bridge," J. Fluid Mech. **341**, 245 (1997).

[19] J. Eggers, "Universal pinching of 3D axisymmetric free-surface flow," Phys. Rev. Lett. **71**, 3458 (1993).

[20] S. Chandrasekhar, *Hydrodynamic and Hydromagnetic Stability* (Dover, New York, 1961).

[21] A. N. Kolmogorov, "On the log normal distribution of the fragment sizes under breakage," Dokl. Akad. Nauk SSSR **31**, 99 (1941).

[22] A. N. Kolmogorov, "On the breakage of drops in a turbulent flow," Dokl. Akad. Nauk SSSR **66**, 825 (1949).

[23] J. E. Mayer and M. G. Mayer, *Statistical Mechanics* (Wiley, New York, 1966).

[24] W. H. Stockmayer, "Theory of molecular size distribution and gel formation in branched-chain polymers," J. Chem. Phys. **11**, 45 (1943).

[25] R. D. Cohen, "Shattering of a liquid drop due to impact," Proc. R. Soc. London, Ser. A **435**, 483 (1991).

[26] M. S. Longuet-Higgins, "The crushing of air cavities in a liquid," Proc. R. Soc. London, Ser. A **439**, 611 (1992).

[27] P. Marmottant, "Atomisation d'un courant liquide dans un courant gazeux," Ph.D. thesis, Institut National Polytechnique de Grenoble, Grenoble, 2001.

[28] M. von Smoluchowski, "Versuch einer theoretische theorie der koagulationskinetik kolloider lsungen," Z. Phys. Chem., Stoechiom. Verwandtschaftsl. **92**, 129 (1917).